Available online at www.sciencedirect.com
ScienceDirect
Applied Catalysis B: Environmental 73 (2007) 209–219
APPLIED CATALYSIS B: ENVIRONMENTAL
www.elsevier.com/locate/apcatb

NO SCR with propane and propene on Co-based alumina catalysts prepared by co-precipitation

Fuxiang Zhang [a], Shujuan Zhang [a,c], Naijia Guan [a,*], Ellen Schreier [b], Manfred Richter [b], Reinhard Eckelt [b], Rolf Fricke [b,*]

[a] *The Institute of New Catalytic Materials Science, Department of Materials Chemistry, Nankai University, Tianjin 300071, PR China*
[b] *Leibniz-Institute for Catalysis, Branch Berlin-Adlershof, PO Box 961156, 12474 Berlin, Germany*
[c] *College of Science, Tianjin University of Science and Technology, Tianjin 300222, PR China*

Received 27 October 2006; received in revised form 13 December 2006; accepted 19 December 2006
Available online 23 December 2006

Abstract

Homogeneous dispersions and small size of deposited high-content cobalt on alumina were achieved by the co-precipitation method and were well maintained on the cobalt-based binary alumina catalysts with Zn, Ag, Fe, Cu or Ni as modifiers. The component and concentration of deposited cobalt species were characterized by UV–vis, EDX and XPS spectra and found to be greatly related to the Co loading, calcination temperatures and the type of additive metals. The optimal Co loading of 8 wt% and calcination temperatures of 800 °C were demonstrated. With respect to the single cobalt-based alumina catalyst, the surface concentration of Co^{2+} on the binary catalysts with addition of Fe, Cu, Ag or Ni was all reduced and accompanying with part conversion of Co^{2+} to Co_3O_4 on the Fe and Ni-modified catalysts. A slight enhanced surface Co^{2+} concentration was only achieved on the Zn-promoted catalyst. It was also demonstrated that for the case of Cu and Fe the additive metals themselves participated in the activation of propene. The octahedral and tetrahedral Co^{2+} ions were suggested as the common active sites. A maximum deNOx activity of 96% was observed on the 8Co4ZnA800 catalyst at the reaction temperatures of 450 °C, and the catalytic performance on the cobalt-based binary alumina catalysts can be described as fellows: CoZn > CoAg, CoNi > Co Cu > CoFe. Based on the *in situ* DRIFT spectra, different reaction intermediates R–ONO and –NCO besides $–NO_2$ were formed on the 8Co4ZnA800 and 8Co4FeA800 samples, respectively, demonstrating their dissimilar reaction mechanisms.

Keywords: Co-precipitation method; High cobalt content; Homogeneous dispersion; NO SCR

1. Introduction

NOx removal from diesel exhaust and oxygen rich fuel gases still remains as one of major challenges in the area of environmental catalysis [1–3]. Various catalysts containing noble metals [4–6], ion-exchanged zeolites [7–9], and metal oxides [10–16] have been extensively reported. Among them, the metal-supported alumina catalysts have received one of the most attentions due to its high activity and stability. It was demonstrated that alumina was a good candidate due to its additional ability for dispersion of transition metal cations [10,14,17].

Among the alumina-based catalysts, Ag/Al_2O_3 [13,24–28], Cu/Al_2O_3 [3,29–32], Au/Al_2O_3 [33,34], Co/Al_2O_3 [10,17,18,35], Pt/Al_2O_3 [36], Sn/Al_2O_3 [38], Fe/Al_2O_3 [39] and Ni/Al_2O_3 [40] have been testified efficient for NO reduction with C_3H_6 as reductant in excess oxygen, and Co/Al_2O_3 has attracted much recent attention due to its good activity and selectivity to nitrogen [10]. It is well known that the deNOx activity is greatly related to the dispersion of cobalt species that are usually influenced by the preparation method, the Co concentration, alumina source, and calcination temperatures [10,17–19,35,41–43]. Octahedrally and tetrahedrally coordinated Co^{2+} ions were considered as main active sites for the SCR activity of NO, while Co_3O_4 was only active for the combustion of hydrocarbon but not for the SCR reaction [43]. High dispersion of Co^{2+} ions with small particle size was thought to be more effective, since more active sites could probably be provided.

* Corresponding authors. Tel.: +86 22 23500341; fax: +86 22 23500341.
E-mail addresses: guannj@nankai.edu.cn (N. Guan), rolf.fricke@catalysis.de (R. Fricke).

0926-3373/$ – see front matter © 2007 Elsevier B.V. All rights reserved.
doi:10.1016/j.apcatb.2006.12.009

Some ways have been suggested to improve the dispersion of Co^{2+} ions and to prevent the aggregation of cobalt particles [10,43,60]. One was to avoid the utilization of a nitrate precursor that tends to facilitate the agglomeration of cobalt species and leads to the formation of unselective Co_3O_4-like particles [10,60]. The other way was to decrease the content of cobalt loading (typically <2–5 wt%) reducing the formation possibility of large particles [10,43]. In addition, high calcination temperatures may be an alternative method, because re-dispersion of large cobalt particles can happen with cobalt aluminate $CoAl_2O_4$ formed at high temperatures [43].

Among all the factors influencing the dispersion and size of deposited cobalt species, the catalyst preparation method was known to be one of the most important. Highly dispersed cobalt species have been prepared by the ion-exchange method [61] and wet-impregnation with acetate complexes [60]. In most of cases, the Co/Al_2O_3 catalysts prepared by a sol–gel method were observed to show much better Co dispersion and relatively better NOx SCR activity than those prepared by impregnation, precipitation and co-impregnation [10,11,19]. However, the cobalt content on these catalysts was usually lower than 2 wt%. To provide much more active sites, the cobalt content of catalyst should be further optimized. For the case of Cu/Al_2O_3, it has been demonstrated [29] that the co-precipitation method can ensure homogeneous dispersion of copper ions and a small size of deposited copper species even when the copper content reached as high as 16 wt%. The high concentrated copper has provided more active sites and caused remarkably enhanced deNOx activity. Accordingly, it is also anticipant to extend the co-precipitation method into the dispersion of cobalt species at high content.

In addition, although high activities and stabilities have been achieved in some cases for Co/Al_2O_3 catalysts [20,21], further improvements are necessary to meet the practical demand of NOx removal. The combination of two catalytic species was testified as an efficient method to further improve the catalytic performance utilizing possible synergistic effects of two metals [19,21–23,37,43]. Unfortunately, the exact effect of additive metal on the cobalt component and dispersion is yet not clear and should be studied more systematically.

In this study, high-loading Zn- (Fe-, Ni-, Cu- or Ag-) promoted Co/Al_2O_3 were prepared via co-precipitation and the effect of additive metals on the selective catalytic reduction (SCR) of NO was systematically examined, where propane and propene were selected as reducing agents. Transmission electron microscopy (TEM), energy-dispersive X-ray analysis (EDX), X-ray diffraction (XRD), X-ray photoelectron spectroscopy (XPS) and UV–vis spectroscopy were employed to characterize the catalysts, and *in situ* diffuse reflectance infrared Fourier transform spectroscopy (DRIFTS) was collected for revealing the mechanism.

2. Experimental

2.1. Catalyst preparation

The cobalt-based alumina binary catalysts were prepared by the co-precipitation method. Fe, Ni, Cu, Zn and Ag were selected as potential promoters. Typically, an aqueous solution containing cobalt nitrate, nickel (or iron, copper, zinc, silver) nitrate and aluminum nitrate was first prepared, and then together with aqueous ammonia (10%) was slowly added into 0.05 mol/L NH_4HCO_3 at room temperature while stirring until the pH of the mother liquor reached about 8. The as-formed co-precipitated hydroxides were filtered and washed with distilled water, dried at 110 °C overnight, and finally calcined at 800 °C for 4 h in static air. According to the content of feed metals and calcination temperatures, the as-prepared particles are denoted as *x*Co*y*MeA*T* (*x* and *y* are the feed content of cobalt and the additive metal separately, "A" means alumina support and *T* stands for the calcination temperatures).

The preparation of Co/Al_2O_3 catalysts was similar, and all of which were denoted as *x*CoA*T*.

2.2. Catalytic tests

The activity measurements were carried out in a fixed-bed stainless steel reactor with an inner diameter of 6 mm. The catalyst powder was compacted to pellets and subsequently crushed yielding samples with mesh sizes of 0.350–0.710 mm. Prior to the reaction, the catalyst was pretreated in the reaction feed gas at 550 °C for 1 h. The feed gas mixture contained 1000 ppm NO, 1000 ppm C_3H_8 or C_3H_6, 5% O_2, and helium as the balance gas. The total gas flow rate was 165 $cm^3\ min^{-1}$ and the catalyst mass was about 0.5 g, resulting in a GHSV of about 10 000 h^{-1}. The reaction temperature has been varied from 350 to 550 °C in steps of 50 K. The composition of the product gas was analyzed by using a gas chromatograph (HP 6890 equipped with Porapak Q and Molecular sieve 5 A columns). A Molecular sieve 5 A column was used for the analysis of N_2, O_2 and CO and a Porapak Q column for analysis of N_2O, CO_2 and C_3H_6. The activity data were collected when the catalytic reaction practically reached steady-state conditions at each temperature chosen. The formation of N_2O was found negligible (<10 ppm) and for this reason this product will not be further discussed in the present study.

2.3. Catalyst characterizations

XRD patterns were collected on a Rigaku D/max 2500 powder diffractometer with Cu Kα radiation equipped with a graphite monochromator. The UV–vis spectrum was recorded on a JASCO V-570 UV–vis spectrophotometer in the range of 220–800 nm. TEM images were acquired on a Tecnai G^2 20 S-TWIN transmission electron microscopy with an accelerate voltage of 200 kV. The as-prepared particles were dispersed in water and dropped onto the surface of a carbon membrane and dried at ambient conditions.

In situ DRIFTS measurements were performed on the spectrometer FTS-60 A (BIO-RAD) by using a diffuse reflectance attachment (HARRICK) equipped with reaction chamber that allows heating under gas flow from room temperature to 500 °C. Two hundred and fifty-six single beam spectra have been co-added at a resolution of 2 cm^{-1}. The spectra are presented as Kubelka–Munk function referred to

the adequate background spectra (sample recorded at the same temperature in He/O_2).

3. Results and discussion

3.1. Characterization of catalysts

As shown in Fig. 1, the 8CoA800 and cobalt-based binary catalysts with different promoting metals and calcination temperatures were examined using transmission electron microscopy (TEM). On all the samples, we can observe the presence of homogeneously dispersed small particles containing Co, as can be more clearly observed in the representative enlarged view of TEM image shown in Fig. 2a. From Fig. 2b, it can be concluded that the size of deposited cobalt is predominantly in the region of 3–5 nm having narrow size distribution. No obvious influences of the additive metal on the cobalt size and dispersion are observed. Different from the 8Co4ZnA800 and 8Co4ZnA1050 catalysts (Fig. 1b and h), most of needle-like compounds are observed on the 8Co4ZnA550 sample (Fig. 1g). This reveals that the state of alumina is related to the calcination temperatures. The energy-dispersive X-ray analysis (EDX) shown in Fig. 2c well indicates the existence of cobalt and of the additive metals on alumina. Determined by the corresponding peak intensities, Table 1 gives the concentrations of cobalt and the additive metals that are all lower than the intended ones. This may be caused by a loss during the preparative process. Because of the use of copper grids during TEM and EDX analysis, all samples reveal traces of copper which does not allow a reliable determination of the Cu concentration of sample 8Co4CuA800.

UV–vis spectra of some Co/Al_2O_3 catalysts were collected to analyze the state of the Co species under ambient conditions, where surface exposed cations are expected to adsorb gas molecules to complete their coordination sphere. The spectra of Co/Al_2O_3 samples with Co concentrations between 2% and 16% calcined at 800 °C (not shown in detail) show a triple at 540, 580 and 625 nm (Fig. 3a for 8CoA800), which can be assigned to the characteristic peaks of tetrahedral Co^{2+} ions [10,42], as found in $CoAl_2O_4$. Compared with 8CoA800, however, the triplet intensities of 8CoA550 is distinctly lower but is similar for the 8CoA1050 sample. A small but distinct peak at 480 nm emerges on all the samples and can be attributed to octahedral Co^{2+} ions [10,17]. With the increase of Co loading, the intensities of characteristic peaks of both tetrahedral and octahedral Co^{2+} ions increase initially and decrease subsequently, and the 8CoA800 sample reaches the maximum. In addition, a broad peak at 310–380 nm appears on samples of 8CoA550, 12CoA800 and 16CoA800, and another broad peak at 700–800 nm only occurs on the 16CoA800 sample. Both of them can be ascribed to the absorption of Co_3O_4 [10,17]. The UV–vis spectra demonstrate that the calcination temperatures and Co loading are two important factors generally influencing the valence state and coordination of cobalt species. The calcination temperature of 800 °C as well as cobalt loading of 8 wt% is desirable for the formation and dispersion of octahedral and tetrahedral Co^{2+} ions here.

As already mentioned by Sachtler and co-workers, a determination of the accurate ratio of octahedral to tetrahedral Co^{2+} ions is very difficult, since the 480 nm peak ($^4T_{1g}(F) \rightarrow {}^4T_{1g}$ (P) transition) is almost two orders of magnitude weaker than the $^4A_2(F) \rightarrow {}^4T_1(P)$ transition of the 540, 580, and 625 nm triplet [10]. According to the peak intensities, the amount of both tetrahedral and octahedral Co^{2+} ions parallel increase first and subsequently decrease with the increasing content of cobalt and calcination temperatures. The 8CoA800 sample reaches the maximum value.

Based on XRD patterns (not shown), no obvious diffraction peaks assigned to the deposited metals or their oxides are observed on all the samples, although the deposited content of

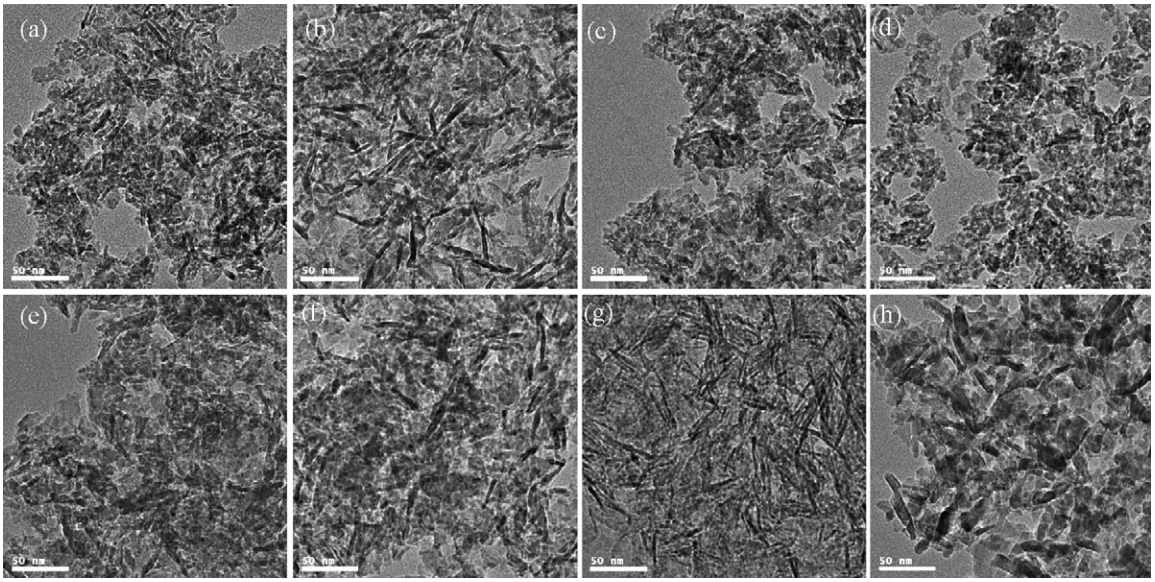

Fig. 1. TEM images of representative catalysts: (a) 8CoA800; (b) 8Co4ZnA800; (c) 8Co4AgA800; (d) 8Co4NiA800; (e) 8Co4CuA800; (f) 8Co4FeA800; (g) 8Co4ZnA550; (h) 8Co4ZnA1050.

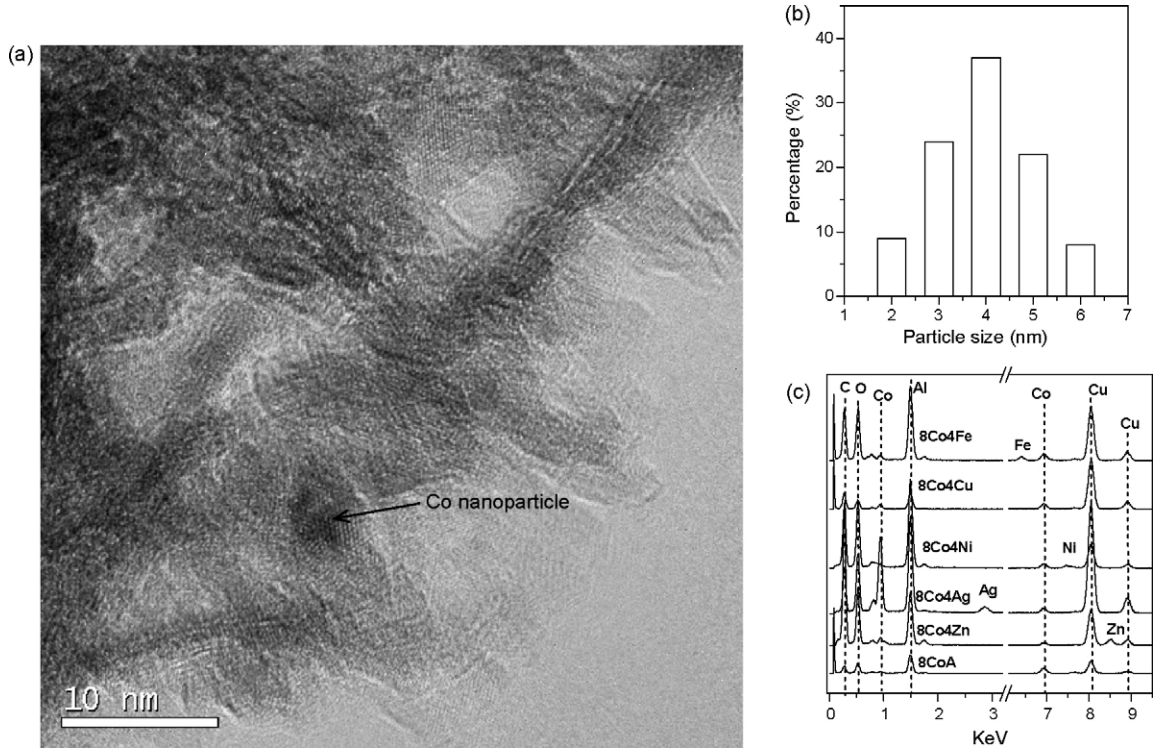

Fig. 2. Enlarged view of typical TEM image (a) and histogram of Co size distribution; (b) of sample 8CoA800; EDX spectra of the cobalt-based catalyst series (c).

cobalt is as high as 8 wt% with the additive metal loading reaching up to 4 wt%. That means, similar to previous copper dispersion [29], the co-precipitation method is definitely beneficial to the homogeneous dispersion of deposited cobalt at high content. The XRD patterns are also well consistent with the TEM observation, in which even dispersion and small size of deposited cobalt species has been observed.

With respect to the 8CoA800 catalysts, the UV–vis spectra of the cobalt-based binary catalysts shown in Fig. 3 are typically different. After the addition of Fe or Cu, the absorption peak intensities of both characteristic tetrahedral Co^{2+} ions at 540, 580 and 625 nm and octahedral Co^{2+} ions at 480 nm become lower compared with the unmodified 8CoA800 sample. For the 8Co4FeA800 and 8Co4NiA800 catalysts, however, emergence of a broad peak at the region of 310–380 nm assigned to the Co_3O_4 species indicates that the addition of Fe or Ni has caused a partial conversion of Co^{2+} ions into Co_3O_4. Both the decreased peak intensity and the formation of Co_3O_4 demonstrate that the additive metals have changed the structure and state of cobalt species.

Table 1
Weight content (wt%) of cobalt and additive metals measured by X-ray photoelectron spectroscopy (XPS) and energy-dispersive X-ray analysis (EDX) as well as the existed state of additive metals deduced from XPS spectra

Sample	Co (%)	XPS[a]		EDX[b]	
		Additive metal		Co (%)	Additive metal (%)
		Content	States		
8CoA	6.9	–	–	7.6	–
8Co4FeA	5.2	1.6	$CoFe_2O_4$	7.4	3.3
8Co4NiA	6	4	NiO	7.5	3.8
8Co4CuA	5.4	3.9	CuO	7.8	–
8Co4ZnA	7.3	2.5	ZnO	7.9	3.4
8Co4AgA	6.3	–	–	7.4	2.9

[a] Metal content within the surface layer.
[b] Metal content in the bulk.

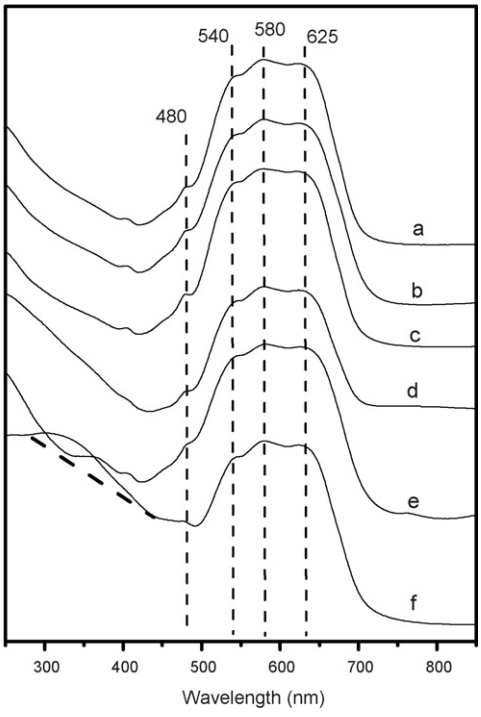

Fig. 3. UV–vis spectra of cobalt-based catalysts:(a) 8CoA800; (b) 8Co4AgA800; (c) 8Co4ZnA800; (d) 8Co4CuA800; (e) 8Co4NiA800; (f) 8Co4FeA800.

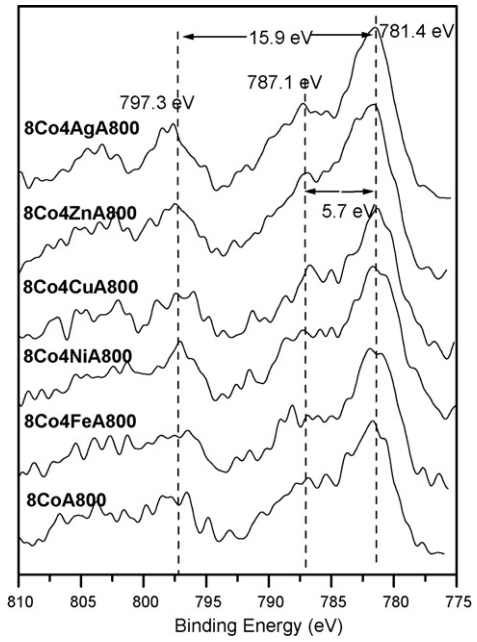

Fig. 4. Co-XPS spectra of the Co/Al_2O_3 and cobalt-based binary catalysts.

As shown in Fig. 4, the Co 2p core level spectra in all the samples are characterized by two components resulting from spin–orbital splitting (Co $2p_{3/2}$ and Co $2p_{1/2}$) and shake-up satellites. It is well known that the spectrum of metallic cobalt commonly does not contain shake-up satellite structure at all [44,45], and the satellite peak of Co^{3+} compounds like Co_3O_4 and Co_2O_3 is usually weak and shifted about 15.0 eV to higher binding energy from their main peak [46]. Accordingly, the observation of spin–orbital splitting between the Co $2p_{3/2}$ and Co $2p_{1/2}$ peaks of ca. 15.9 eV and strong satellite lines located at about 5.7 eV allow us to describe the chemical state of cobalt as Co^{2+} ions (CoO, $Co(OH)_2$ and $CoAl_2O_4$) and to exclude practically the existence of Co^{3+} ions and metallic cobalt [46]. Nevertheless, the predominant Co species here should be CoO and $CoAl_2O_4$, since $Co(OH)_2$ will be decomposed into CoO at the calcination temperatures of 800 °C. This is well in agreement with the results of UV–vis spectra that tetrahedral and octahedral Co^{2+} was primarily observed on these samples. Although the UV–vis spectra of the samples 8Co4FeA800 and 8Co4NiA800 demonstrated the formation of Co_3O_4, the XPS spectra ruled out the existence of Co^{3+} ions, indicating that the Co_3O_4 species may rather exist in the bulk of the catalyst than on the outer surface.

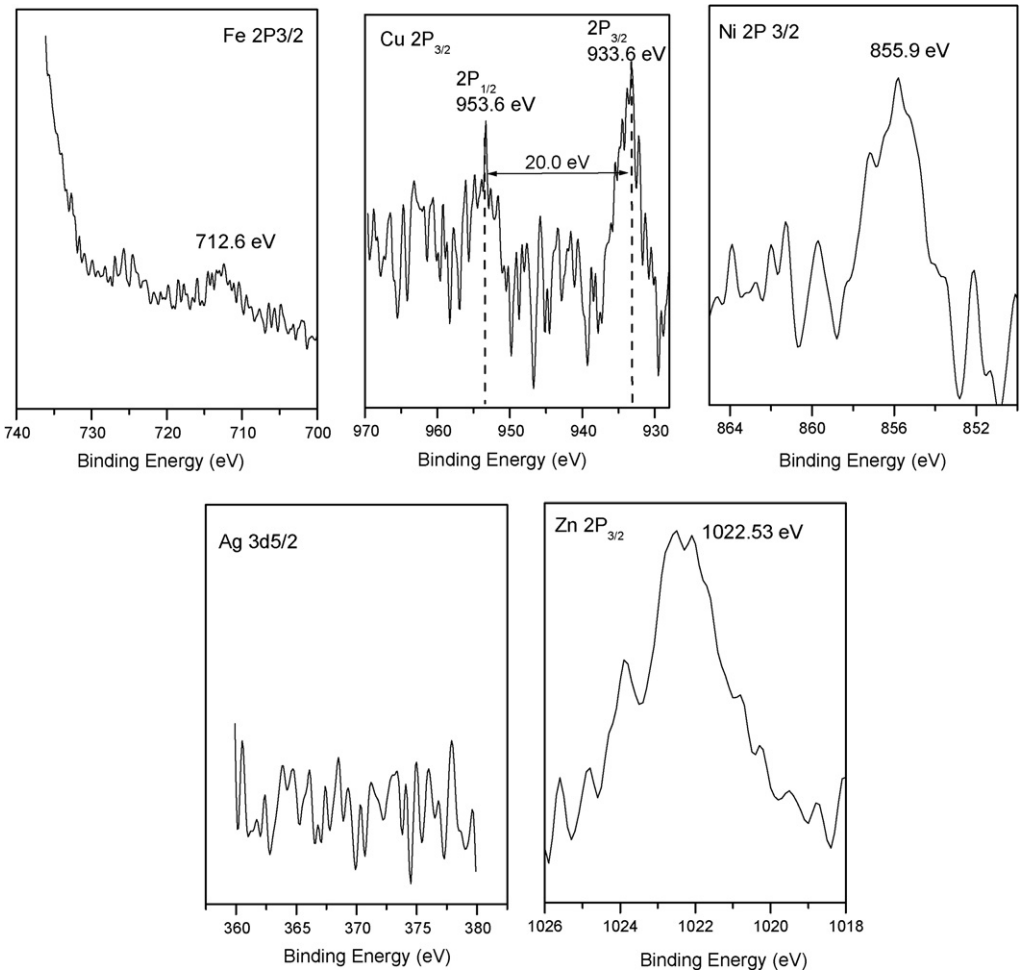

Fig. 5. XPS spectra of additive metals on the cobalt-based binary catalysts with calcination temperatures of 800 °C (8Co4MeA800).

The state of second metal Fe, Cu, Ni and Zn can be determined as $CoFe_2O_4$ [47,48], CuO [49], NiO [50] and ZnO [51], respectively, according to their corresponding binding energy of XPS spectra as shown in Fig. 5, and all the species were given in Table 1. The determination of CuO species was also from the satellite peaks of Cu $2p_{1/2}$ at 953.6 eV with binding energy difference of 20.0 eV to the main peak Cu $2p_{3/2}$ at 933.6 eV. It should be emphasized, however, that, in particular, in the near-alumina region the formation of spinels cannot be excluded. For 8Co4AgA800 catalyst, no obvious silver 3d spectra are observed, demonstrating the absence of silver on the surface of catalyst. Both the formation of $CoFe_2O_4$ and the lack of silver on the surface of catalysts indicate that a strong interaction between cobalt and the additive metals iron and silver appears.

According to the intensities of the corresponding core level XPS lines (Al 2p, O 1s, Co 2p, Fe 2p, Ni 2p, Cu 2p, Zn 2p and Ag 3d), the weight content of Co and additive metals can be determined and is summarized in Table 1. One can see that the surface Co concentration was diminished by Fe, Ni, Ag and Cu, and among them the influence of Fe on the concentration of Co in the surface-near region (as determined by XPS) is the most remarkable, in particular, because its concentration is the lowest. A possible reason for this effect might be the formation of $CoFe_2O_4$ spinels. A slight increase of surface Co species is only observed over the 8Co4ZnA800 catalyst. The changes of the cobalt concentration indicate that the additive metals generally influence the dispersion of Co species on the surface of catalysts.

3.2. Catalytic performance

3.2.1. The unmodified Co/Al_2O_3 catalyst

Preparation method, Co concentration and calcination temperatures applied were considered to be important factors for their structure and dispersion that commonly influence the catalytic performance. Concerning the optimal Co concentration there still exists a disagreeing discussion in the literatures [10,11,18,19,41]. As to the impregnation method, Hamada et al. [41] reported the optimal Co loadings at 0.1 wt% with the NO conversion of 55% at 450 °C, while Horiuchi et al. [18] found the optimal NO conversion catalyst at a Co loading of 0.5 wt%. Similarly, for Co/Al_2O_3 catalysts prepared by sol–gel method, Hamada et al. found the highest NO conversion of 88–90% at the temperature of 350–400 °C for a Co loading of 0.8–1.8 wt% [11]. However, other authors have reported an optimal activity for catalysts with a higher Co loading up to 2 wt% [10,19]. Therefore, cobalt content and calcination temperatures of Co/Al_2O_3 catalysts were optimized in a first step before examining the effect of additive metals using propane as reductant to avoid superimposition by coking effects.

Table 2 compares the catalytic activities of NO with propane as reducing agent on the series of Co/Al_2O_3 catalysts. At higher reaction temperatures, the 8CoA800 sample is more effective than other catalysts with different Co loading and calcination temperatures, showing the best conversion of 90.3% at the reaction temperature of 500 °C. At the same Co loadings (series 8CoAT) but applying different post-calcination temperatures (T = 550, 800, and 1050 °C), it becomes obvious that up to a reaction temperature of 400 °C a low calcination temperature to 550 °C (sample 8CoA550) gives the highest conversion degrees for NO. Although, this sample shows also high conversion degrees at higher reaction temperature, an increase of the calcination temperature to 800 °C (sample 8CoA800) is advantageous to obtain maximum conversion degrees. Calcination at 1050 °C produces a catalyst which shows always lower activity than the other two catalysts with 8 wt% Co.

Table 2
NO-SCR by propane as a function of reaction temperature over Co/Al_2O_3 catalysts with different Co contents and calcination temperatures[a]

Catalyst	Conversion (%)				
	350 °C	400 °C	450 °C	500 °C	550 °C
2CoA800	2.5	10.0	58.7	72.7	64.7
4CoA800	4.0	20.0	63.7	82.0	72.0
8CoA800	10.5	24.2	74.0	90.3	77.8
12CoA800	14.7	34.7	72.0	79.3	60.0
16CoA800	16.0	38.0	53.7	72.0	38.0
8CoA550	16.7	63.7	69.0	78.0	59.0
8CoA1050	3.0	8.0	31.3	74.0	68.0

[a] Reaction conditions: 1000 ppm NO, 1000 ppm C_3H_8, 5% O_2, balance He; GHSV = 10 000 h^{-1}.

It is interesting that all the cobalt catalysts with metal concentrations of 2–16 wt% and calcination temperatures of 800 °C show good activities at 500 °C varying from 72.0% to 90.3%. These results completely differ from those results achieved on catalysts prepared by the sol–gel and the impregnation method, where the authors have shown that higher Co loading (above 2 wt%) lead to decreased activities of catalysts and even deactivation [10,11,18,19,41]. The good catalytic performance of the present Co-containing catalysts at high Co content should be attributed to the high dispersion and small size of deposited cobalt species on alumina caused by the co-precipitation method, providing much more active sites.

Tetrahedral and octahedral Co^{2+} ions have been primarily considered as the active sites, even though there is still some debate concerning the exact structure of the active site [10,29,52]. In this study, the changes of deNOx activities on the catalysts with different Co loading and calcination temperatures are greatly related to the variation of the concentration of surface Co^{2+} ions that first increases and subsequently decreases. Compared with the 8CoA800 sample, less amount of octahedral and tetrahedral Co^{2+} ions are observed on the other catalysts. Moreover, Co_3O_4-like species are simultaneously formed on the 8CoA550, 12CoA800 and 16CoA800 samples, which were known to be mainly active for the oxidation of propane instead of NO leading to the decreased selectivity of propane to the formation of nitrogen [10,43]. Accordingly, due to the observed parallel development of the Co^{2+} signal (UV–vis) and the catalytic activity, Co^{2+} is considered to be the active species for NO reduction. However, since the concentration of tetrahedral and octahedral Co^{2+} ions changes similarly with the cobalt content and calcination temperatures, it remains difficult to differentiate between these

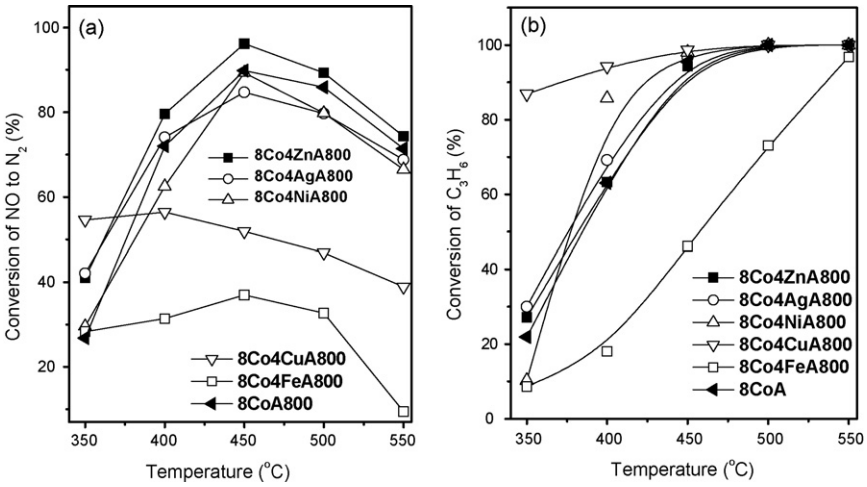

Fig. 6. Conversion of NO and C_3H_6 on various cobalt-based binary catalysts at different reaction temperatures: (a) NO conversion and (b) C_3H_6 conversion. Reaction conditions: NO = 1000 ppm; C_3H_6 = 1000 ppm; O_2 = 5%; GHSV = 10 000 h^{-1}.

coordinations and to determine which of these is the main active site.

3.2.2. *The modified Co–Me/Al_2O_3 catalysts*

After the optimization stage for the single component Co/Al_2O_3, the feed composition was changed and propane was replaced by propene for the study of the Co–Me/Al_2O_3 catalyst series. As known from numerous reports in literature propene is easier to activate resulting in a shift of the activity curve to lower temperatures, where the study of possible additive effects might be facilitated. The conversions of NO and C_3H_6 on the cobalt-based binary catalysts are shown in Fig. 6. Compared to the reductant propane, the conversion degree of NO to N_2 is similar, however, the activity curve is clearly shifted to lower reaction temperatures. In detail, the maximum conversion reaches about 90% already at 450 °C with propene compared to 500 °C with propane.

The influence of the ad-metal can be divided into the following way: (i) the addition of Cu and Fe, leading to a decreased conversion of NO; (ii) the presence of Ag and Ni, which has no distinct effect on the NO conversion; and (iii) an obvious promoting effect observed for Zn (Figs. 6 and 7). It can also be seen from Fig. 7a that the conversion of NO on 8Co4ZnA800 catalyst is much superior to that of a Zn/Al_2O_3 catalyst (4ZnA800) which has been prepared for comparison. This effect is also observed for the activation of propene (Fig. 7b), where, different from the NO conversion, the combination of Co and Zn shows no advantage in the propene activation. This might be explained by oxidation of most of propene to CO_x.

Different from the NO activity curves, the conversions of C_3H_6 on the binary catalysts all increase with enhanced reaction temperatures (Fig. 6b). Among them, the 8Co4CuA800 catalyst shows the highest activity for the hydrocarbon oxidation, while the 8Co4FeA800 catalyst has the lowest activity. With respect to the sample 8CoA800, all catalysts other than 8Co4FeA800 and 8Co4CuA800 show a slight deviation in the conversion of propene; but all reach 100% conversion at temperatures higher than 500 °C.

A comparison of Fig. 6a and b allows some conclusions on the low performance of catalysts 8Co4CuA800 and

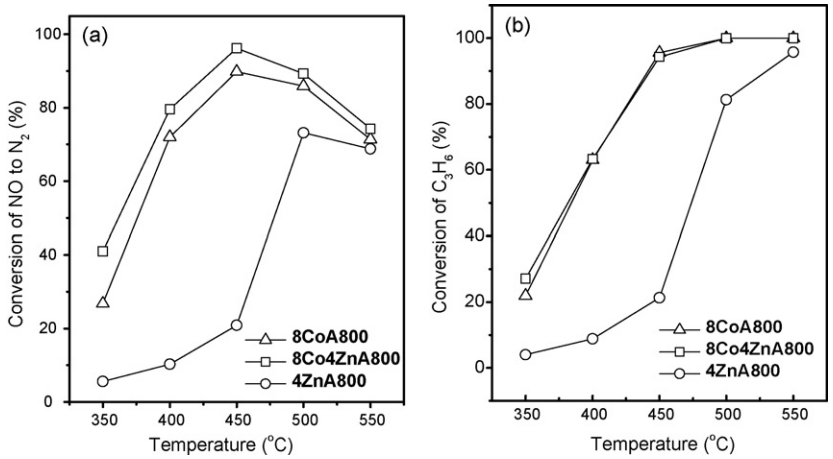

Fig. 7. Conversion of NO and C_3H_6 on 8CoA800, 4ZnA800 and 8Co4ZnA800 catalysts at different reaction temperatures: (a) conversion of NO and (b) conversion of C_3H_6. Reaction conditions: NO = 1000 ppm; C_3H_6 = 1000 ppm; O_2 = 5%; GHSV = 10 000 h^{-1}.

8Co4FeA800. In all catalysts, Co is the main component and is expected to determine the catalytic performance where the ad-metals are introduced to modify these properties. As shown in Fig. 6a this holds particularly for the addition of Zn, where the degree of NO conversion is increased. In the cases of Cu and Fe, a negative effect is observed because the NO conversion drastically decreased when these metals are additionally introduced. The reason for this behavior becomes obvious from the results of propene conversion (Fig. 6b). First, it is obvious that Cu shows a very high oxidation power for propene. This results in a nearly complete combustion of propene already at temperatures as low as 350 °C (Fig. 6b). The participation of propene in the reduction of NO is, therefore, rather limited. Surprisingly, the opposite holds for the Fe-modified catalyst where propene is only slowly converted even at temperatures up to 500 °C. As a result, low activity of NO reduction with propene is observed.

Concerning Ag and Ni the Co^{2+} concentration (estimated from the UV–vis spectral intensities, Fig. 3) as well as the activation of propene do not differ very much from the unmodified catalyst 8CoA800. The degree of NO conversion in dependence on temperature is nearly identical for these samples.

Different from the other additives, the contribution of zinc on the 8Co4ZnA800 can be expected to mainly promote the surface dispersion of Co^{2+} ions (Table 1) and subsequently cause the slight increase of propene consumption.

It has been demonstrated that the deNOx activity with hydrocarbon as reductant was predominantly determined by the activation of both NO and hydrocarbon, and a high selectivity in the use of hydrocarbon for the formation of reduced forms of nitrogen was required for achievement of high catalytic activity [43]. The activation of NO and hydrocarbon were primarily related to the concentration of Co^{2+} ions as the active centers, and suitable activation of the hydrocarbon was desirable to enhance its selectivity for the conversion of NO to nitrogen [10,43]. Accordingly, the decrease of surface Co^{2+} ions as well as the inhibition of propene activation on the 8Co4FeA800 sample

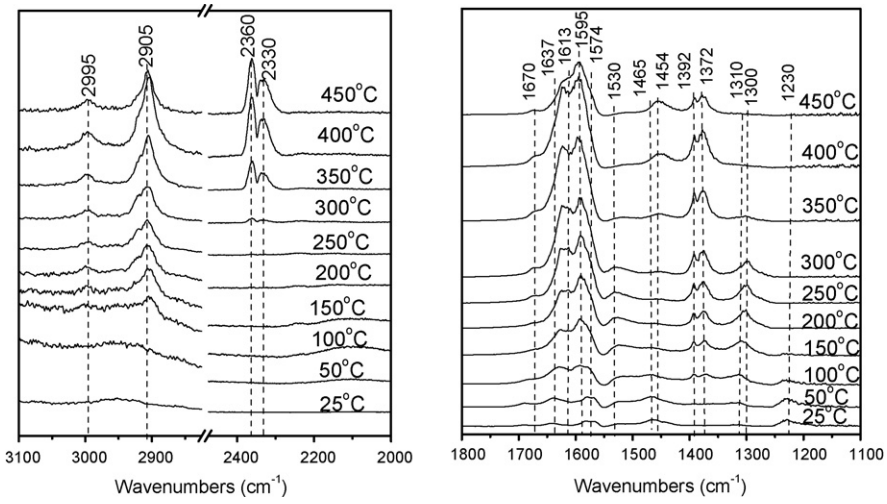

Fig. 8. *In situ* DRIFTS on the 8Co4ZnA800 sample at various temperatures. Feed: 1000 ppm NO + 1000 ppm C_3H_6 + 10% O_2/He.

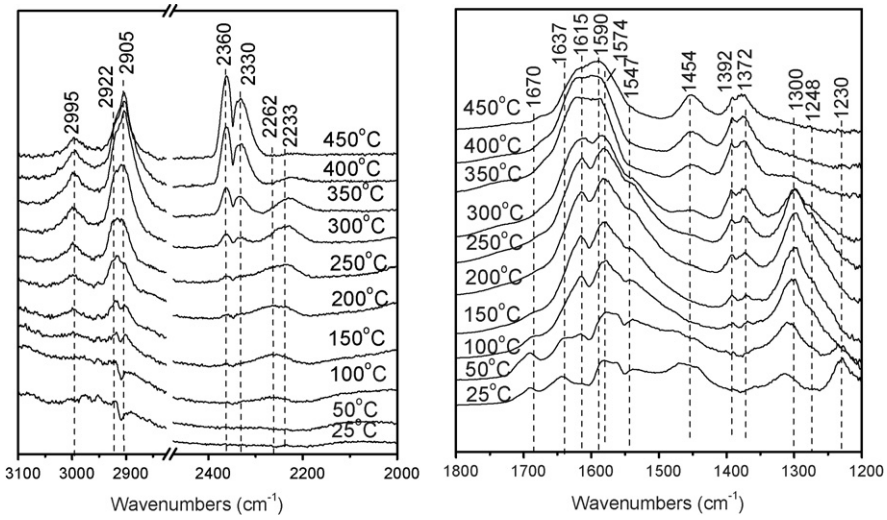

Fig. 9. *In situ* DRIFTS on the 8Co4FeA800 sample at various temperatures. Feed: 1000 ppm NO + 1000 ppm C_3H_6 + 10% O_2/He.

should be responsible for the poor deNOx performance. As to the 8Co4CuA800 catalyst, the lower concentrated surface Co^{2+} ions decrease the NO activation. On the other hand, the rapid activation of propene will decrease the selectivity for the formation of nitrogen. The integrated effect of decreased NO activation and selectivity of propene for the formation of nitrogen leads to the lower deNOx activity. Different from the effect of Cu and Fe, the content of Co^{2+} ions and activation of propene on the 8Co4NiA800 and 8Co4AgA800 catalysts are more close to that on the 8CoA800 sample, so the deNOx activities on them are comparable. Owing to the enhanced surface Co^{2+} ions dispersion as well as the suitable activation of propene, the deNOx activity on the 8Co4ZnA800 sample is obviously promoted. Summarizing, the different deNOx activities on the cobalt-based binary catalysts should be the integrated result of the activation of NO and the combustion efficiency of propene.

3.3. *In situ* DRIFTS of the NO reduction over 8Co4ZnA800 and 8Co4FeA800

In situ DRIFTS on the 8Co4ZnA800 and 8Co4FeA800 showing the highest and lowest activity were investigated as an attempt to wonder whether the differences in activity are reflected in properties of the DRIFT spectra or not. The DRIFTS spectra recorded in the steady state at various temperatures are shown in Figs. 8 and 9. The sample was exposed to a gas mixture of $NO/C_3H_6/O_2/He$ from 25 to 450 °C with a heating ramp of 5 K/min.

After the exposure of the 8Co4ZnA800 catalyst to the feed ($NO + C_3H_6 + O_2$ mixture) gas for 8 min at room temperature, some IR peaks appear in the region between 1700 and 1100 cm^{-1}, as shown in Fig. 8. According to previous literature [53], the weak bands at 1230 and 1465 cm^{-1} can be attributed to bidentate or chelating nitrite NO_2^- and linear nitrite NO_2^-. When the temperature increased to 200 °C, all IR peaks attributed to nitrite species decrease. Simultaneously, bands are developed at 1300 cm^{-1} attributed to monodentate nitrate NO_3^- and at 1613 cm^{-1} assigned to bridging nitrate NO_3^- [54]. This shows that an oxidation of nitrite species to nitrate species has taken place. At 300 °C a part of C_3H_6 was oxidized to CO_2 which is accompanied with the appearance of bands at 2330 and 2360 cm^{-1} [53]. The bands at 2905, 1595, 1392 and 1372 cm^{-1} can be ascribed to formate species, and those at 1454 and 1574 cm^{-1} to acetate formed at about 300 °C [53,57–59]. Bands which appear at 2905 and 2995 cm^{-1} in the CH stretching vibration region are related to an adsorbed hydrocarbon fragment. The peak at 1637 cm^{-1} can be assigned to enolic surface species ($C{=}C{-}O^-$) [57]. At 400 °C no bands are observed due to adsorbed nitrate species, only carboxylate species are evidenced. The strong bands at 1670, 1595 and 1392 cm^{-1} can be attributed to ν(–ONO), ν(–NO_2) and δ(–CH_3), respectively, indicating that organic compounds $C_xH_yNO_z$ (R–ONO and R–NO_2) are largely formed on the catalyst surface [53,59]. The detailed attachment of the IR spectra can be referred to Table 3.

Fig. 9 shows the IR spectra of the 8Co4FeA800 catalyst in the flow of $NO + C_3H_6 + O_2$ in the steady state at various temperatures. Compared with Fig. 8, the bands at 1300, 1454, 1574, 1392, 1590 and 1670 cm^{-1} can similarly be assigned to the characteristic bands of nitrates, acetate, R–NO_2, and

Table 3
Bands observed on Co–Zn–Al_2O_3 catalyst during *in situ* DRIFTS experiments and corresponding surface species and vibrations to which they were assigned

Wavenumber (cm^{-1})	Surface species	Vibration	Reference
1230	Bidentate or chelating nitrite NO_2^-	ν^a_{ONO}	[53]
1298	Monodentate nitrate NO_3^-		[54]
1304	Bidentate nitrate NO_3^-	ν_{ONO}	[55]
1310	Bidentate nitrate NO_3^-	ν^a_{ONO}	[53]
1320	Monodentate nitrite NO_2^-		[53]
1465	Linear nitrite NO_2^-		[53]
1547	Chelating bidentate nitrate species		[56]
1250/1550	Nitrate "A" NO_3^-	$\nu_{N=O}$	[53]
1556	Monodentate nitrate NO_3^-	$\nu_{N=O}$	[55]
1567	Bidentate nitrate NO_3^-		[53]
1580	Monodentate nitrate NO_3^-		[57]
1616	Bridging nitrate NO_3^-	ν_{ONO}	[54]
1372	Formate $HCOO^-$	δ_{CH}	[58,59]
1392	Formate $HCOO^-$	δ_{CH}	[53,58]
1460/1454	Free carboxylate COO^-/acetate	ν^s_{OCO}	[53,57,59]
1575/1562	Free carboxylate COO^-/acetate	ν^a_{OCO}	[53,57,59]
1590	Aromatics, polyene, acrylate?		[53]
1595	Formate $HCOO^-$	ν^a_{OCO}	[53]
1637	Enolic structure (partial oxidation of C_3H_6) CH_2CHO^-		[57]
2230–2250	isocyanate –NCO	ν^s_{OCO}	[53]
2330	Carbon dioxide CO_2(g)		[53]
2360	Carbon dioxide CO_2(g)		[53]
2905	Formate $HCOO^-$	ν_{CH}	[53]
1662/1651	Organic nitrito-compound (R–ONO)	ν_{ONO}	[53,59]
1593	Organic nitro-compound (R–NO_2)	ν_{NO_2}	[53,59]

s: symmetric, a: asymmetric, ν: stretching, δ: bending.

R–ONO species, respectively. The primary difference between Figs. 8 and 9 is the emergence of a new peak on the 8Co4FeA800 sample at 2233 cm^{-1}, which has been assigned to isocyanate (–NCO) surface species regarded as a key intermediate species by many researchers [55,57–59]. With increasing temperatures, the bands of nitrate (1300 cm^{-1}) decrease promptly, while the –NCO (2233 cm^{-1}) and $–NO_2$ (1590 cm^{-1}) bands progressively appear. This may indicate that the –NCO and $–NO_2$ species are possibly reaction intermediates.

Compared with the reaction mechanism proposed by Meunier et al. [53] for the SCR of NO by C_3H_6 over Co/Al_2O_3 catalysts which included R-ONO and R-NO_2 species as the key intermediates, the *in situ* DRIFT spectra observed on the Zn-promoted Co/Al_2O_3 catalyst (Fig. 8) are very similar, indicating that the addition of Zn has not obviously changed the reaction mechanism. For the 8Co4FeA800 catalyst, however, the appearance of other intermediate species, such as, –NCO and $–NO_2$, indicates that the reaction mechanism on the Fe-promoted catalyst is different from that on the 8CoA800 and 8Co4ZnA800 samples. Moreover, the peak intensities of adsorbed species on 8Co4FeA800 catalyst are significantly weaker than that observed on the 8Co4ZnA800 catalyst. Accordingly, the different reaction mechanism as well as the decreased intensities of adsorbed species may be another reason for the observation of lower activity on the Fe-promoted catalyst.

Burch et al. [43] have published a simplified scheme of the mechanism of the propene-SCR of NO to N_2 over oxide catalysts. According to their idea several inorganic NO_x species (e.g. nitrates), hydrocarbon species (e.g. acetate) contribute to the first step of reaction. In the second step different nitrogen compounds are formed from which R–CN, R–NCO, R–NH_2, and NH_3 are suggested to be involved into the final formation of N_2. Our DRIFT spectra also support this concept with the exception that no evidence has been found that the R–CN species are stable intermediates.

4. Conclusions

The Co-precipitation method is definitely beneficial to the homogeneous dispersion and aggregation prevention of deposited high-concentrated cobalt on alumina, and the uniform morphology and small size of deposited cobalt were well maintained under the presence of Fe, Ni, Cu, Zn or Ag. Suitable cobalt loading (8 wt%) and calcination temperatures (800 °C) are desirable for the formation of tetrahedral and octahedral Co^{2+} ions suggested as the common active sites. Additive metals have a moderate influence on the surface concentration of cobalt species, whereas the conversion of hydrocarbons is not affected. The effect of Cu and Fe on the NO_x conversion is outstanding possibly due to fast oxidation of propene and the formation of $CoFe_2O_4$ spinels. The different deNOx activities on the cobalt-based binary catalysts was ascribed to the integrated effect of the activation of NO and the combustion efficiency of propene. An obvious promotion effect was only observed for the zinc addition, and the modification effect of additive metals can be described as follows: CoZn > CoAg, CoNi > CoCu > CoFe. Maximum NO conversion of 96% was achieved at the reaction temperatures of 450 °C on the 8Co4ZnA800 sample. Due to a probable formation of $CoFe_2O_4$ spinel the reaction on the Fe promoted cobalt catalyst was dissimilar to that on the Co/Al_2O_3 and Zn-promoted samples.

Acknowledgements

This work was financially supported by the Deutsche Forschungsgemeinschaft (DFG), Germany; the National Natural Science Foundation of China (Grant Nos. 20233030 and 20573059, 20603019), and National Basic Research Program of China (also called 973) with Grant No. 2003CB615801.

References

[1] M. Shelef, Chem. Rev. 95 (1995) 209.
[2] R. Burch, Catal. Rev. 46 (2004) 271.
[3] R. Hernández-Huesca, J. Santamaría-González, P. Braos-García, P. Maireles-Torres, E. Rodríguez-Castellón, A. Jiménez-López, Appl. Catal. B 29 (2001) 1.
[4] H. Hamada, Y. Kintaichi, M. Sasaki, T. Ito, Appl. Catal. 75 (1991) 1.
[5] R. Burch, P.J. Millington, Catal. Today 29 (1996) 37.
[6] H. Ohtsuka, Appl. Catal. B 33 (2001) 325.
[7] M. Iwamoto, H. Yahiro, S. Shundo, Y. Yu-u, N. Mizuno, Appl. Catal. 69 (1991) 15.
[8] Y. Li, J.N. Armor, J. Catal. 145 (1994) 1.
[9] L.L. Ren, T. Zhang, D.B. Liang, C.H. Xu, J.W. Tang, L.W. Lin, Appl. Catal. B 35 (2002) 317.
[10] J.Y. Yan, M.C. Kung, W.M.H. Sachtler, H.H. Kung, J. Catal. 172 (1997) 178.
[11] T. Maunula, J. Ahola, H. Hamada, Appl. Catal. B 26 (2000) 173.
[12] K.A. Bethke, H.H. Kung, J. Catal. 172 (1997) 93.
[13] E. Seker, J. Cavataio, E. Gulari, P. Lorpongpaiboon, S. Osuwan, Appl. Catal. A 183 (1999) 121.
[14] M.C. Kung, P.W. Park, D.-W. Kim, H.H. Kung, J. Catal. 181 (1999) 1.
[15] P.W. Park, H.H. Kung, D.-W. Kim, M.C. Kung, J. Catal. 184 (1999) 440.
[16] T. Miyadera, K. Yoshida, Chem. Lett. (1993) 1483.
[17] L.F. Liotta, G. Pataleo, A. Macaluso, G. Di Carlo, G. Deganello, Appl. Catal. A 245 (2003) 167.
[18] T. Horiuchi, T. Fujiwara, L. Chen, K. Suzuki, T. Mori, Catal. Lett. 78 (2002) 319.
[19] L. Chen, T. Horiuchi, T. Mori, Catal. Lett. 72 (2001) 71.
[20] A. Obuchi, I. Kaneko, J. Oi, A. Ohi, A. Ogata, G.R. Bamwenda, S. Kushiyama, Appl. Catal. B 15 (1998) 37.
[21] Z. Liu, J. Hao, L. Fu, T. Zhu, J. Li, X. Cui, Appl. Catal. B: Environ. 48 (2004) 37.
[22] M. Haneda, Y. Kintaichi, H. Hamada, Catal. Today 54 (1999) 391.
[23] I.H. Son, M.C. Kim, H.L. Koh, K.-L. Kim, Catal. Lett. 75 (2001) 191.
[24] K. Shimizu, J. Shibata, H. Yoshida, A. Satsuma, T. Hattori, Appl. Catal. B: Environ. 30 (2001) 151.
[25] F.C. Meunier, J.P. Breen, V. Zuzaniuk, M. Olsson, J.R.H. Ross, J. Catal. 187 (1999) 493.
[26] K. Takagi, T. Kobayashi, H. Ohkita, T. Mizushima, N. Kakuta, A. Abe, K. Yoshida, Catal. Today 45 (1998) 123.
[27] F.C. Meunier, J.R.H. Ross, Appl. Catal. B: Environ. 24 (2000) 23.
[28] X. She, M.F. Stephanopoulos, J. Catal. 237 (2006) 79.
[29] K. Shimizu, H. Maeshima, A. Satsuma, T. Hattori, Appl. Catal. B 18 (1998) 163.
[30] S. Junji, S. Ken-ichi, S. Atsushi, H. Tadashi, Appl. Catal. B: Environ. 37 (2002) 197.

[31] L. Chen, H. Tatsuro, T. Osaki, M. Toshiaki, Appl. Catal. B: Environ. 23 (1999) 259.
[32] E. Seker, N. Yasyerli, E. Gulari, C. Lambert, R.H. Hammerle, J. Catal. 208 (2002) 15.
[33] F.C. Meunier, R. Ukropec, C. Stapleton, J.R.H. Ross, Appl. Catal. B 30 (2001) 163.
[34] A. Ueda, M. Haruta, Appl. Catal. B: Environ. 18 (1998) 115.
[35] A. Sarellas, D. Niakolas, K. Bourikas, J. Vakros, C. Kordulis, J. Colloid Interface Sci. 295 (2006) 165.
[36] A.A. Nikolopoulos, E.S. Stergioula, E.A. Efthimiadis, I.A. Vasaos, Catal. Today 54 (1999) 439.
[37] M. Richter, M. Langpape, S. Kolf, G. Grubert, R. Eckelt, J. Radnik, M. Schneider, M.-M. Pohl, R. Fricke, Appl. Catal. B: Environ. 36 (2002) 261.
[38] M. Ozawa, H. Toda, S. Suzuki, Appl. Catal. B: Environ. 8 (1996) 141.
[39] S.C. Shen, S. Kawi, Appl. Catal. B 45 (2003) 63.
[40] A.Z. Ma, M. Muhler, W. Grünert, Appl. Catal. B 27 (2000) 37.
[41] H. Hamada, Y. Kintaichi, M. Inaba, M. Tabata, T. Yoshinari, H. Tsuchisa, Catal. Today 29 (1996) 53.
[42] G.N. Asmolov, O.V. Krylov, Kinet. Catal. 12 (1971) 403.
[43] R. Burch, J.P. Breen, F.C. Meunier, Appl. Catal. B 39 (2002) 283.
[44] N.S. McIntyre, M.G. Cook, Anal. Chem. 47 (1975) 2208.
[45] K.S. Chung, F.E. Massoth, J. Catal. 64 (1980) 320.
[46] A.A. Khassin, T.M. Yurieva, V.V. Kaichev, V.I. Bukhtiyarov, A.A. Budneva, E.A. Paukshtis, V.N. Parmon, J. Mol. Catal. A: Chem. 175 (2001) 189.
[47] T.B. Scott, G.C. Allen, P.J. Heard, M.G. Randell, Geochim. Cosmochim. Acta 69 (24) (2005) 5639.
[48] X. Yang, X. Wang, Z. Zhang, J. Cryst. Growth 277 (2005) 467.
[49] D.W. Zeng, K.C. Yung, C.S. Xie, Appl. Surf. Sci. 217 (2003) 170.
[50] Z. Hou, O. Yokota, T. Tanaka, T. Yashima, Appl. Surf. Sci. 233 (2004) 58.
[51] H.S. Liu, T.S. Chin, S.W. Yung, Mater. Chem. Phys. 50 (1997) 1.
[52] N. Okazaki, S. Tsuda, Y. Shiina, A. Tada, M. Iwamoto, Chem. Lett. 5 (1998) 429.
[53] F.C. Meunier, V. Zuzaniuk, J.P. Breen, M. Olsson, J.R.H. Ross, Catal. Today 59 (2000) 287.
[54] B. Westerberg, E. Fride, J. Mol. Catal. A 165 (2001) 249.
[55] J. Wang, Y. Yu, S. Xie, H. He, Chin. J. Catal. 25 (2004) 824.
[56] B.I. Mosqueda-Jiménez, A. Jentys, K. Seshan, J.A. Lercher, Appl. Catal. B 46 (2003) 189.
[57] H. He, J. Wang, Q. Feng, Y. Yu, K. Yoshida, Appl. Catal. B 46 (2003) 365.
[58] K. Shimizu, H. Kawabata, H. Maeshima, A. Satsuma, T. Hattori, J. Phys. Chem. B 104 (2000) 2885.
[59] Y. Chi, S.S.C. Chuang, Catal. Today 62 (2000) 303.
[60] M. Inaba, Y. Kintaichi, M. Haneda, H. Hamada, Catal. Lett. 39 (1996) 269.
[61] B. Djonev, B. Tsyntsarski, D. Klissurski, K. Hadjiivanov, J. Chem. Soc., Faraday Trans. 93 (1997) 4055.